20.9 A 1.92mW Filtering Transimpedance Amplifier for RF Current Passive Mixers

Tian Ya Liu, Antonio Liscidini

University of Toronto, Toronto, ON, Canada

Nowadays, current passive mixers represent the state of the art for signal down-conversion in wireless receivers. In such kind of structures, noise, distortions and losses are strictly correlated to the performance of the stage following the mixer. The most common solution adopted to sense the down-converted current is a transimpedance amplifier (TIA) in shunt with a capacitance to ground that assures a low input impedance when the loop gain of the amplifier decreases (Fig. 20.9.1a). A low input impedance is necessary to have a small voltage swing at the output of the mixer (typically few hundreds mV) to minimize the modulation of the switch resistance and with it the distortion produced during the downconversion. The input capacitance can also be used to filter the majority of the out-of-band interferers by transforming the TIA into a filter [1,2] (Fig. 20.9.1b). This reduces the dynamic range required by the TIA and its power consumption. This advantage comes at a cost of area, since the limited voltage swing tolerable at the input of the TIA demands a large capacitor to absorb the downconverted interferers. This trade-off is relaxed with the proposed solution (Fig. 20.9.2), where the input capacitance (C1) is partially boosted by a feedback network minimizing the swing required at the input of the TIA. This idea, originally proposed in [3] only to improve the 1dB compression point, is now used to maximize the spurious-free dynamic range of the TIA, exploiting an intrinsic in-band highpass shaping of noise and distortion. Furthermore, an adaptive transfer function, which improves its filtering action in presence of large out-of-band interferers, is realized.

The basic idea in this paper is to build a lowpass filter where the memory elements (i.e. the capacitors) are placed in the feedback network instead of the feedforward path. To obtain a 2nd-order lowpass profile, the feedback network must have two real zeros, which become complex poles in the closed loop transfer function [3]. In the scheme in Fig. 20.9.2, the zeros, one at DC and one at 1/R2C2, are implemented by C1 and C2-R2 in feedback with an operational transconductance amplifier (OTA), respectively. In the filter passband, the feedback loop is open and the circuit works as a conventional TIA with a transresistance gain equal to R1. On the contrary, in the filter stopband, C1 is boosted by draining the interferers (I_{INT}) before entering in the virtual ground of the TIA (I_{TIA}). In theory, C1 can absorb out-of-band interferers even without any voltage swing at the input of the TIA, which ensures a low input impendence to improve the linearity of the passive mixer. Furthermore, since one of the terminals of C1 is connected to the feedback network, it can easily swing rail-to-rail and the size of the capacitor required to absorb a given input current becomes much smaller compared to the solutions presented in [1,2], where the voltage swing across the input capacitor is limited to a few hundreds of mV. A small grounded capacitance is still present at the TIA input (Fig. 20.9.2) to absorb the far-away interferers at frequencies for which the loop gain drops.

Another important feature of the TIA is an intrinsic highpass shaping of the noise and the distortion produced by the feedback network. This property is derived from the presence of the zeros in the feedback that behave as open circuits in the filter passband, therefore preventing the injection of noise and distortion. As shown in Fig. 20.9.3, both the noise and the distortion produced by R2 and by the transconductor benefit from a 20dB/dec highpass shaping until the filter cut-off frequency. The OTA can be implemented with a simple CMOS transconductor biased in Class-AB (Fig. 20.9.3). Since the intermodulation products, generated in the filter passband by out-of-band interferers, are filtered, the stage can be biased in Class-AB to save power without compromising the overall linearity of the TIA. The noise shaping also allows scaling the impedance level of the feedback network reducing the area required by the elements of the filter.

The Class-AB operation of the transconductor results in a TIA unique property of having an adapting filtering profile as a function of the magnitude of the input signal. The finite OTA transconductance (gm) introduces a couple of complex conjugate poles in the feedback network (Fig. 20.9.3), which result in a couple of complex zeros in the closed-loop transfer function. Since the OTA is biased with a small DC current to operate in Class-AB, in absence of large interferers it exhibits a small gm, which sets the zeros at low frequency, thus limiting the filter attenuation. However, in presence of a large interferer, the OTA operates in Class-AB with a higher large-signal transconductance that moves the zeros to higher frequencies, thus improving the selectivity. This characteristic changes the TIA properties automatically as a function of the operative scenario without the need of any control loop, therefore adding a degree of freedom in the design optimization.

A fully differential TIA based on the scheme in Fig. 20.9.2 was integrated in a 0.13µm IBM CMOS technology. The frequency range of the channel-selection filter was set between 2.8 and 12MHz to address cellular applications. As explained in [4], the cut-off frequency of the filter was chosen larger than the channel bandwidth to benefit from the presence of the highpass shaping of noise and distortion. The TIA was tested by feeding a signal with a voltage signal generator in series with a resistance of 1.6kΩ to emulate the finite output resistance of a passive mixer (as done in [4]). The active area of the design is 0.45mm^2, dominated by the capacitors (104pF). The total capacitance used at the input is 56pF, 28pF capacitors are used for the two ground capacitors and 28pF for the two C1s. The remaining 48pF are present in the feedback network. In the narrowest band (2.8MHz), it was possible to reach a differential input impedance lower than 150Ω after one octave from the cut-off frequency (i.e. 5.6MHz), to ensure a limited voltage swing even in the presence of large interferers (some mA). To have comparable input impedance and cut-off frequency, the filtering TIAs in [1,2] would have required a differential input capacitance greater than 200pF (almost 4× more than used in this design).

The reconfigurability is obtained by tuning the capacitive elements of the filter (including the input grounded capacitance, tuned for the lowest band). The OTA was biased with 400µA in order to place the zeros one decade above the cut-off frequency to keep the in-band filter response independent of the out-of-band interferer magnitude. Figure 20.9.4a shows the filter transfer functions measured with a small input current (40µA) in order to have the OTA operating in Class-A. In the narrowest band, the presence of the zeros (due to the finite transconductance of the OTA) reduce the selectivity of the filter. Although the zeros should produce a flat response above 28MHz, a 5dB-peaking occurs due to the finite bandwidth of the TIA. The peaking further reduces the selectivity but does not compromise the stability since the phase margin is maintained above 30 degrees in all corners. When the response is measured with a larger input signal (Fig. 20.9.4b), the zeros are pushed to higher frequencies because the OTA starts operating in Class-AB. This automatically removes the peaking and improves the selectivity up to 13dB. Notice that for a larger bandwidth the zeros are already at a higher frequency and their effect is mitigated by the presence of the input grounded capacitors.

Figure 20.9.5 shows the high pass-shaping of the 3rd-order intermodulation product (IM3) generated in the filter passband due to the presence of two out-of-band interferers. The measurement (shown for the lowest cut-off frequency) was done by placing a one tone at 10MHz and by moving down the other one from 20MHz in order to sweep IM3 over the entire filter passband. All the other measurement results and the die micrograph are reported in Fig. 20.9.6 and Fig. 20.9.7, respectively. The overall current consumption for the two sets of measurements is 1.6mA under a 1.2V voltage supply, leading to an overall power consumption of 1.92mW. For the largest bandwidth, the linearity is dominated by the feedforward path and decreases due to the finite gain-bandwidth product of the operational amplifier. In order to compare this solution with the state of the art of continuous-time filters, the FOM defined in [5] is used and reported in the Fig. 20.9.6. Thanks to the highpass shaping of noise and distortion, the obtained FOM varies between 176dB(J^{-1}) and 182dB(J^{-1}).

References:

[1] M.-D. Tsai et al., "A Multi-Band Inductor-less SAW-less 2G/3G-TD-SCDMA Cellular Receiver in 40nm CMOS," *ISSCC Dig. Tech. Papers*, pp. 354-355, Feb. 2014.

[2] I. Fabiano et al., "SAW-less Analog Front-End Receivers for TDD and FDD," *ISSCC Dig. Tech. Papers*, pp.82-83, Feb. 2013.

[3] A. Perez-Carrillo et al., "A large-signal blocker robust transimpedance amplifier for coexisting radio receivers in 45nm CMOS," *IEEE Radio Frequency Integrated Circuits Symp.,* pp. 1-4, June 2011

[4] A. Pirola et al., "Current-Mode, WCDMA Channel Filter with In-Band Noise Shaping," *IEEE J. Solid-State Circuits*, vol. 45, no. 9, pp. 1770–1780, Sept. 2010.

[5] W. Sansen, "Analog design challenges in nanometer CMOS technologies," *IEEE Asian Solid-State Circuits Conf.*, pp. 5–9, Nov. 2007.

 978-1-4673-9467-3/16/$31.00

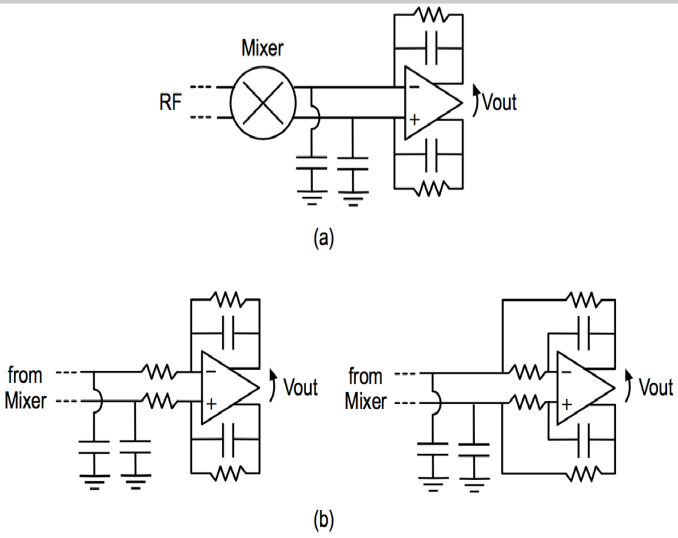

Figure 20.9.1: a) Traditional TIA approach b) 2nd-order filtering TIA topologies [1,2].

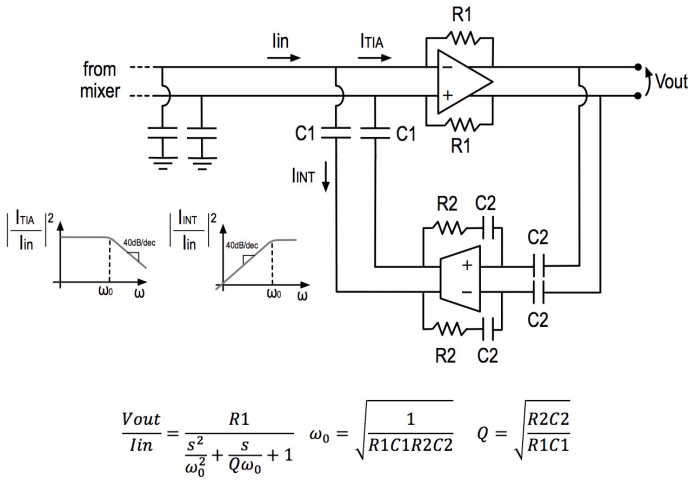

$$\frac{Vout}{Iin} = \frac{R1}{\frac{s^2}{\omega_0^2} + \frac{s}{Q\omega_0} + 1} \qquad \omega_0 = \sqrt{\frac{1}{R1C1R2C2}} \qquad Q = \sqrt{\frac{R2C2}{R1C1}}$$

Figure 20.9.2: Proposed filtering TIA with zeros in the feedback network.

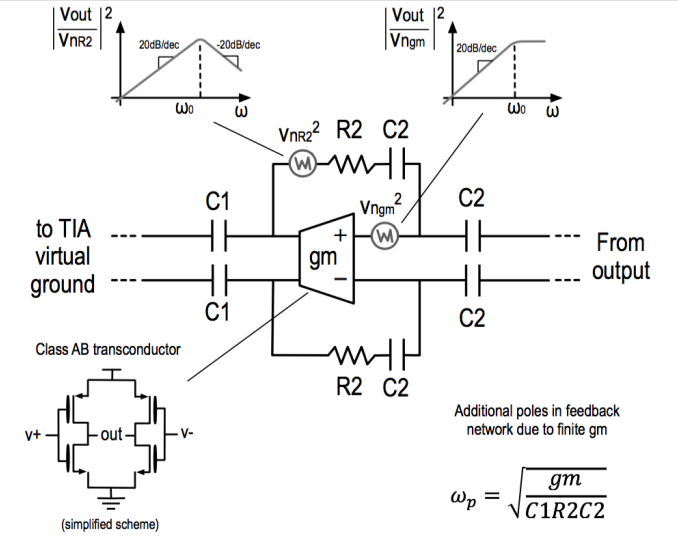

$$\omega_p = \sqrt{\frac{gm}{C1R2C2}}$$

Figure 20.9.3: Feedback network details: noise shaping, Class-AB transconductor, additional poles due to finite gm.

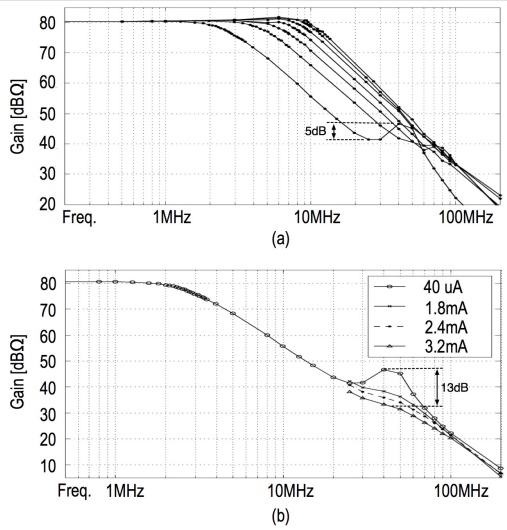

Figure 20.9.4: a) TIA transfer functions (cut-off 2.8 to 12MHz), b) Transfer function for different levels of input current signal.

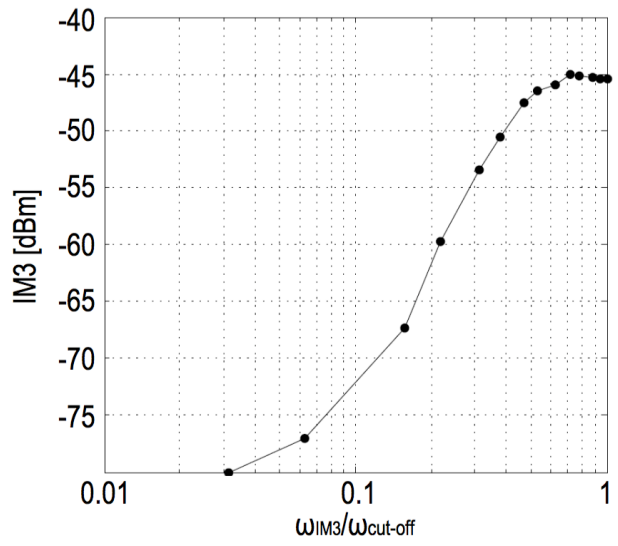

Figure 20.9.5: Output IM3 in-band highpass shaping.

	Lowest Band	Highest Band
Technology (µm)	0.13	
Voltage Supply [V]	1.2	
DC Power [mW]	1.92	
Number of poles (n)	2	
Cut-off (f_{-3dB}) [MHz]	2.8	12
IIP3 out of band [dBm]*	48.5	36.1
Input Referred Noise [μV_{RMS}]**	18.4	33.1
SFDR out of band [dB]	86.8	75.1
Area (mm^2)	0.45	
FOM [$dB(J^{-1})$]	182	176

* Tones at 10MHz and 19.5MHz (lowest band), 50MHz and 95MHz (highest band)

** Integrated in the channel bandwidth 1.92MHz (WCDMA) and 10MHz (LTE20)

$$FOM = 10\,Log\,\frac{SFDR \cdot n \cdot f_{-3dB}}{Power}$$

Figure 20.9.6: Summary of measurement results.

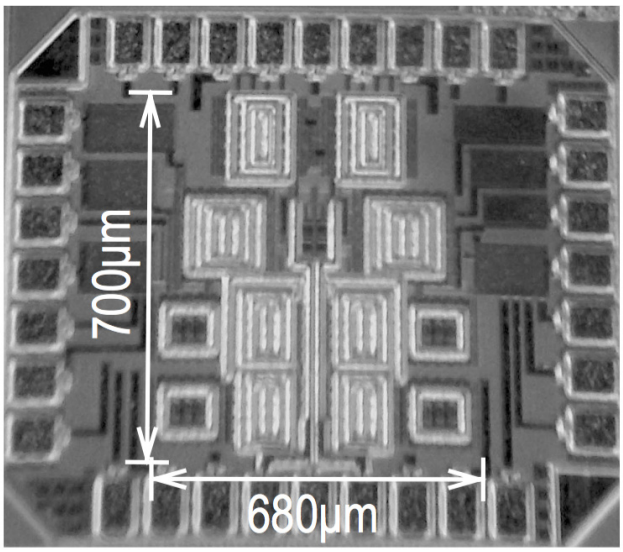

Figure 20.9.7: Die micrograph.

978-1-4673-9467-3/16/$31.00